

## Asymptotic Analysis of Lattice Boltzmann Outflow Treatments

Michael Junk and Zhaoxia Yang\*

*FB Mathematik und Statistik, Universität Konstanz, Postfach D194,  
78457 Konstanz, Germany.*

Received 9 October 2009; Accepted (in revised version) 29 September 2010

Available online 24 December 2010

---

**Abstract.** We show the methodology and advantages of asymptotic analysis when applied to lattice Boltzmann outflow treatments. On the one hand, one can analyze outflow algorithms formulated directly in terms of the lattice Boltzmann variables, like the extrapolation method, to find the induced outflow conditions in terms of the Navier-Stokes variables. On the other hand, one can check the consistency and accuracy of lattice Boltzmann outflow treatments to given hydrodynamic outflow conditions like the Neumann or average pressure condition. As example how the gained insight can be used, we propose an improvement of the well known extrapolation method.

**AMS subject classifications:** 65N06, 76D05, 82C40

**Key words:** Outflow condition, asymptotic analysis, lattice Boltzmann method.

---

### 1 Introduction

In contrast to conventional CFD methods where the fluid velocity and pressure are primary variables, the lattice Boltzmann method recovers them as averages of the mesoscopic particle distributions in a postprocessing step (see, for example, [1, 8, 9, 12, 15, 21–23]). The advantage of very simple evolution equations for the particle distributions, however, come at the price of non-transparent relations between the desired hydrodynamic boundary conditions and the required lattice Boltzmann boundary treatments. In this article, we show that asymptotic analysis can help to clarify this relationship.

The standard lattice Boltzmann method is comprised of two phases, a collision phase and a transport phase

$$f^c(n, \mathbf{j}) = f(n, \mathbf{j}) - A(f - f^{eq})(n, \mathbf{j}), \quad (1.1a)$$

$$f_i(n+1, \mathbf{j} + \mathbf{c}_i) = f_i^c(n, \mathbf{j}). \quad (1.1b)$$

---

\*Corresponding author. *Email addresses:* michael.junk@uni-konstanz.de (M. Junk), zhaoxia.yang@uni-konstanz.de (Z. Yang)

Here,  $f(n, \mathbf{j})$  is the vector of particle distribution functions  $f_i(n, \mathbf{j}) = f(n, \mathbf{j}, \mathbf{c}_i)$  at the  $n$ th time level  $t_n$  and the lattice node  $\mathbf{x}_j$  ( $\mathbf{j} \in \mathbb{Z}^d$ ) with the discrete velocity  $\mathbf{c}_i \in \{-1, 0, 1\}^d$  ( $i = 1, 2, \dots, N$ ). The particles collide locally, which is modeled with a linear operator  $A$  including BGK [23] and MRT [9, 20] approaches. The equilibrium functions  $f_i^{eq}$  recommended in [12] are adopted here,

$$f_i^{eq} = F_i(\hat{\rho}, \hat{\mathbf{u}}), \quad F_i(\hat{\rho}, \hat{\mathbf{u}}) = f_i^* \left( \hat{\rho} + 3\hat{\mathbf{u}} \cdot \mathbf{c}_i + \frac{9}{2} (\hat{\mathbf{u}} \cdot \mathbf{c}_i)^2 - \frac{3}{2} |\hat{\mathbf{u}}|^2 \right), \quad (1.2)$$

in which

$$\hat{\rho} = \sum_{i=1}^N f_i, \quad \hat{\mathbf{u}} = \sum_{i=1}^N \mathbf{c}_i f_i \quad (1.3)$$

are the mass density and the average momentum of the particles based on the assumption that the fluid density slightly fluctuates around a constant  $\bar{\rho}$  (here,  $\bar{\rho} = 1$  without loss of generality). The constants  $f_i^*$  depend on the chosen velocity model.

The Chapman-Enskog expansion [2, 10, 11, 13] and asymptotic analysis [17, 18, 27] show that for incompressible flows governed by the Navier-Stokes equations,

$$\nabla \cdot \mathbf{u} = 0, \quad \partial_t \mathbf{u} + (\mathbf{u} \cdot \nabla) \mathbf{u} + \nabla p = \nu \nabla^2 \mathbf{u}, \quad \mathbf{u}|_{t=0} = \boldsymbol{\psi}, \quad (1.4)$$

the fluid velocity  $\mathbf{u}$  and pressure  $p$  can be extracted from the lattice Boltzmann moments  $\hat{\rho}$  and  $\hat{\mathbf{u}}$  with second order accuracy, supposing that the eigenvalues of the collision matrix  $A$  are properly related to the fluid shear viscosity  $\nu$  and that initial and boundary conditions are approximated sufficiently accurate.

As far as boundary conditions are concerned, we can distinguish two basic types. (1) The Navier-Stokes problem (1.4) includes certain hydrodynamical boundary conditions (like no-slip velocity conditions, or normal stress conditions). Then, the task is to find consistent lattice Boltzmann boundary algorithms, which comes with the general difficulty that the required lattice Boltzmann boundary conditions outnumber the given hydrodynamical ones. The additional conditions have to be chosen very carefully in order to avoid conflicts on the hydrodynamical level which entail poor approximations. (2) The solution domain of (1.4) is very large or unbounded (like pipe flows or exterior flows). Then, for numerical reasons, artificial boundaries have to be introduced where no obvious physical boundary conditions are available. Again, one way to proceed is to adopt outflow conditions formulated in terms of the hydrodynamical variables and construct associated lattice Boltzmann algorithms (like the Neumann condition for the fluid velocity  $\mathbf{u}$  [19], the do-nothing condition [19], the average pressure condition [25], or the convective condition on  $\mathbf{u}$  [26]). Another way is to formulate reasonable outflow conditions directly for the lattice Boltzmann variables (like the extrapolation method [28], the approximation by using Grad's moments [3] and the convective condition on  $f_i$  [16, 28]). If this approach is successful, the implied conditions on the hydrodynamical level may be a valuable alternative to existing outflow treatments.

Whichever scenario has to be dealt with, it is clear that an analytical tool is required to extract the hydrodynamical boundary conditions hidden in a given lattice Boltzmann algorithm. In this article, we want to show that such a tool is available and that it generates valuable insight into lattice Boltzmann algorithms which naturally leads to modifications and improvements. As examples to illustrate the method, we choose two outflow boundary conditions: the extrapolation method [28] and the do-nothing condition [19].

## 2 Asymptotic analysis

A brief outline of the asymptotic analysis in the case of lattice Boltzmann BGK models (where, formally,  $A = I/\tau$  is a multiple of the identity) is given below. A detailed discussion for general collision matrices  $A$  can be found in [17, 18, 27]. The lattice Boltzmann solutions  $f_i$  are assumed to have regular expansions

$$f_i(n, \mathbf{j}) = f_i^{(0)}(t_n, \mathbf{x}_j) + h f_i^{(1)}(t_n, \mathbf{x}_j) + \dots, \quad (2.1)$$

where  $h$  is the grid size. The coefficients  $f_i^{(k)}$  are sufficiently smooth functions with respect to  $t$  and  $\mathbf{x}$  and independent of  $h$ . We insert these expansions into the lattice Boltzmann update rule (1.1), do Taylor expansion at the fluid grid points and sort the terms with equal powers of  $h$ . Then the coefficients  $f_i^{(k)}$  can be found order by order and a prediction  $\hat{f}_i$  of the lattice Boltzmann solution  $f_i$  can be constructed

$$\hat{f}_i = f_i^{(0)} + h f_i^{(1)} + \dots + h^4 f_i^{(4)}, \quad (2.2)$$

where

$$f_i^{(0)} = f_i^*, \quad (2.3a)$$

$$f_i^{(1)} = 3f_i^* \mathbf{c}_i \cdot \mathbf{u}, \quad (2.3b)$$

$$f_i^{(2)} = f_i^* \left( 3p + \frac{9}{2} (\mathbf{c}_i \cdot \mathbf{u})^2 - \frac{3}{2} \mathbf{u}^2 \right) - \tau \mathbf{c}_i \cdot \nabla f_i^{(1)}, \quad (2.3c)$$

$$f_i^{(3)} = 3f_i^* \mathbf{c}_i \cdot \mathbf{w} - \tau \left( \partial_t f_i^{(1)} + (\mathbf{c}_i \cdot \nabla) f_i^{(2)} + \frac{1}{2} (\mathbf{c}_i \cdot \nabla)^2 f_i^{(1)} \right), \quad (2.3d)$$

$$f_i^{(4)} = f_i^* \left( 3q + \frac{9}{2} (\mathbf{c}_i \cdot \mathbf{u}) (\mathbf{c}_i \cdot \mathbf{w}) - \frac{3}{2} (\mathbf{u} \cdot \mathbf{w}) \right) - \tau \left( \partial_t f_i^{(2)} + (\mathbf{c}_i \cdot \nabla) f_i^{(3)} + \frac{1}{2} (\mathbf{c}_i \cdot \nabla)^2 f_i^{(2)} + D(\partial_t, \mathbf{c}_i \cdot \nabla) f_i^{(1)} \right), \quad (2.3e)$$

and  $D$  in the expression for  $f_i^{(4)}$  is some third order polynomial. While the zeroth order coefficient  $f_i^{(0)}$  is simply constant, the first and second order coefficients depend on the Navier-Stokes variables  $\mathbf{u}$  and  $p$ , showing a clear relationship between leading order contributions to the lattice Boltzmann variables and the hydrodynamic quantities. This relationship is the basis for constructing boundary conditions which are formulated in terms of  $p$ ,  $\mathbf{u}$ , or derivatives of  $\mathbf{u}$ .

The detailed analysis also shows that the additional vector field  $w$  appearing in the third order contribution and the scalar field  $q$  appearing in fourth order satisfy a non-homogeneous Oseen type equation with a source term depending on the Navier-Stokes solution. In general, the higher order contributions  $w$  and  $q$  do not vanish which entails that the Navier-Stokes quantities  $u$  and  $p$  can at best be extracted up to error terms of order  $h^2$  from the analytic prediction  $\hat{f}_i$  via

$$\mathbf{u} = \frac{1}{h} \sum_{i=1}^N \mathbf{c}_i \hat{f}_i + \mathcal{O}(h^2), \quad p = \frac{1}{h^2} \left( \sum_{i=1}^N \hat{f}_i - 1 \right) + \mathcal{O}(h^2). \quad (2.4)$$

Since  $\hat{f}_i$  is close to the numerical solution  $f_i$  of the lattice Boltzmann update rule (1.1), one can conclude that second order in the grid size  $h$  is the optimal accuracy of the Navier-Stokes solution obtained from the standard lattice Boltzmann algorithm.

However, the accuracy order may decline due to incompatible initial or boundary conditions. To analyze the influence of these conditions, we insert the prediction functions  $\hat{f}_i$  into the initial and boundary algorithms, do Taylor expansion at intersection points between grid lines and the boundary and sort terms of equal order in  $h$ . Again, the leading order of the residues expose the hydrodynamic initial and boundary conditions corresponding to the lattice Boltzmann algorithm as well as the consistency order and the expected accuracy. The success of this idea has been demonstrated in detail with the asymptotic analysis of velocity Dirichlet conditions [18]. In the following section, we apply the idea to the analysis of outflow treatments.

### 3 Analysis of outflow treatments

The benchmark problem which we use to investigate the behavior of different outflow treatments is the classical non-stationary 2D flow around a cylinder with Reynolds number  $Re = 100$ .

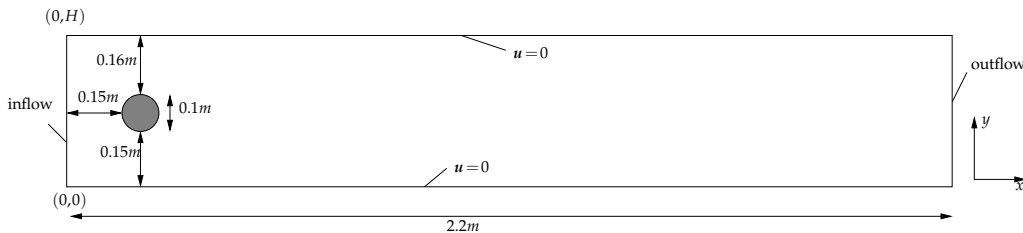


Figure 1: Configuration of the 2D test case from [24].

The detailed configuration of this flow can be found in [24] together with reference values for the drag and lift coefficients  $C_d$ ,  $C_l$  and the pressure difference  $\Delta p$  at the cylinder (see also Fig. 1). This helps to investigate the influence of the outflow condition on the inner flow. Behind the cylinder, a continuous vortex shedding occurs (Fig. 2).

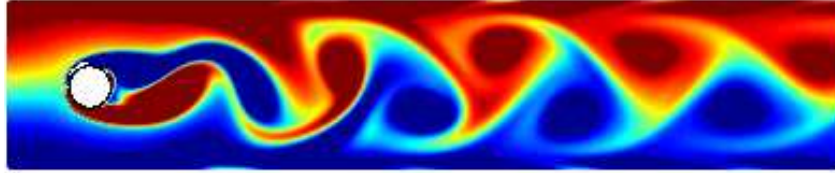


Figure 2: The vortex shedding behind the cylinder is displayed by plotting the curl of the fluid velocity.

A qualitative requirement on an outflow condition is that the vortices pass through the outlet as if the channel had infinite length. Practically, we compare the flow fields from simulations with fixed channel width but varying length (the length-width ratio  $(L/H)$  ranges in  $\{2,3,5\}$ ) and take the degree of variation as indicator for the quality of the outflow treatment.

### 3.1 Do-nothing condition

The do-nothing condition [14] is an open boundary condition suggested for the incompressible Navier-Stokes equation,

$$-pn + \nu \frac{\partial \mathbf{u}}{\partial \mathbf{n}} = 0. \quad (3.1)$$

The notion "do-nothing" refers to the facts that it is obtained as a natural boundary condition from a particular variational formulation of the Navier-Stokes equation (for details and derivation see [7, 14]).

With the help of the asymptotic expansion and the resulting structural information on the variables  $f_i$  and their relation to  $p$  and the derivatives of  $\mathbf{u}$ , a lattice Boltzmann implementation of (3.1) has been constructed in [19]. When the outer normal direction  $\mathbf{n}$  is opposite to one of the incoming velocity directions  $\mathbf{c}_i$ , the algorithm treats the lattice Boltzmann variable  $f_i$  different from the variables for the other incoming velocities

$$f_i(n+1, j_o) = \left[ F_i^{eq}(\mathbf{1}, \hat{\mathbf{u}}) - \left( \frac{V}{\tau} - 1 \right) f_{i^*}^{neq} \right] (n, j_o), \quad \mathbf{c}_i = -\mathbf{n}, \quad (3.2a)$$

$$f_i(n+1, j_o) = f_{i^*}^c(n, j_o + \mathbf{c}_i) + 6f_i^* [\hat{u}_x(n, j_o)c_{ix} + \hat{u}_y(n, j_o - \mathbf{n})c_{iy}], \quad \mathbf{c}_i \neq -\mathbf{n}. \quad (3.2b)$$

Here,  $j_o$  is the label of a boundary node,  $i^*$  is the index of the discrete velocity  $\mathbf{c}_{i^*} = -\mathbf{c}_i$ ,  $\mathbf{f}^{neq} = \mathbf{f} - \mathbf{f}^{eq}$  is the non-equilibrium part of the distribution function, and  $\hat{u}_x, \hat{u}_y$  are the normal and tangential components of the velocity  $\hat{\mathbf{u}}$ .

In order to verify analytically that the algorithm (3.2a), (3.2b) realizes condition (3.1), we insert the prediction  $\hat{f}_i$  with coefficients (2.3) into (3.2a). Then a Taylor expansion is carried out around the node  $(t_n, \mathbf{x}_{j_o})$  which leads to

$$h^2 3f_i^* (p - \nu(\mathbf{n} \cdot \nabla)(\mathbf{u} \cdot \mathbf{n})) = \mathcal{O}(h^3), \quad (3.3)$$

where  $c_i = -\mathbf{n}$  has been used. A detailed specification of the next order coefficient is possible. It depends on time derivatives of the Navier-Stokes flow velocity and does not vanish for general flows. Dividing by  $3f_i^*h^2$ , we thus find

$$-p + \nu \frac{\partial \mathbf{u} \cdot \mathbf{n}}{\partial \mathbf{n}} = \mathcal{O}(h). \quad (3.4)$$

The scheme (3.2b) produces similarly

$$h^2 6f_i^* (\mathbf{n} \cdot \nabla) (\mathbf{u} \cdot \mathbf{t}) c_{iy} = \mathcal{O}(h^3), \quad (3.5)$$

which leads to

$$\frac{\partial \mathbf{u} \cdot \mathbf{t}}{\partial \mathbf{n}} = \mathcal{O}(h). \quad (3.6)$$

Multiplying (3.4) by  $\mathbf{n}$  and (3.6) by  $\mathbf{t}$  and adding up finally yields

$$-p\mathbf{n} + \nu \frac{\partial \mathbf{u}}{\partial \mathbf{n}} = \mathcal{O}(h), \quad (3.7)$$

which tell us that the boundary algorithm (3.2a), (3.2b) is consistent to the do-nothing condition with first order accuracy.

Since the do-nothing condition is natural in a weak formulation [14] and has proved to produce reasonable results, its lattice Boltzmann implementation is also expected to behave reasonably. In fact, the numerical simulations of the channel flow demonstrate that this outflow treatment does not influence the inner flow significantly, as long as  $L/H$  is large enough.

The numerical results reported in Fig. 3 correspond to aspect ratios  $L/H \in \{2, 3, 5\}$ . Especially with the rather small ratios  $L/H = 2, 3$  one cannot expect to obtain a precise solution. However, our goal is to demonstrate the influence of the outflow condition on the inner flow which is, of course, more drastic when the ratio changes from 5 to 2 than from 8 to 5. This is due to the fact that, close to the cylinder, the gradients of the flow fields are stronger. For the same reason, the small ratio  $L/H = 2$  acts as a stability check of the outflow condition because strong gradients are more likely to trigger instabilities than weaker gradients further away from the cylinder.

In Fig. 3, the three lower plots show cross sections of the velocity and pressure fields along the center line of the channel. One can observe that the profiles for different channel lengths are close to each other which supports that the do-nothing condition allows to substitute a longer channel by a shorter one without drastic influence on the general structure of the solution. A more detailed inspection of the solution in terms of lift and drag coefficients as well as pressure difference between front and back of the cylinder shows bigger variations which is not surprising due to the higher sensitivity of these functionals and the comparably short channel lengths. For drag and lift, the maxima of the signal should be in the interval indicated by the dashed horizontal lines which is satisfied for the reasonable case  $L/H = 5$ . As explained above, with smaller ratios it is unlikely to obtain high precision.

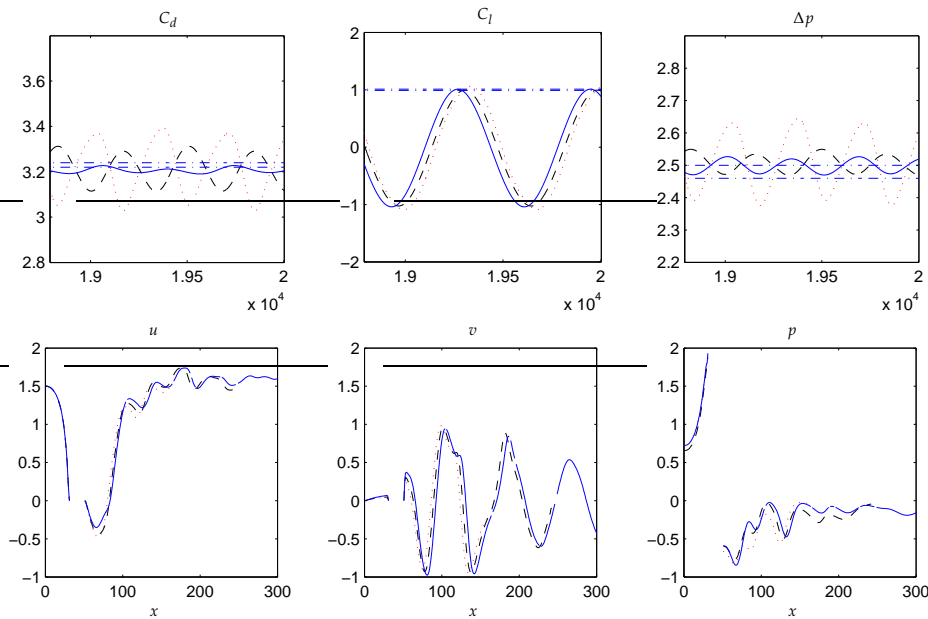


Figure 3: The simulation results obtained with the do-nothing condition are demonstrated by the dotted lines ( $L/H=2$ ), dashed lines ( $L/H=3$ ) and solid lines ( $L/H=5$ ). The upper plots show how the drag ( $C_d$ ), lift ( $C_l$ ) coefficients and the pressure difference at the cylinder ( $\Delta p$ ) vary in 2000 time steps (from 18000 to 20000). The dash-dotted lines display the interval of the reference values. The lower plots are the velocity and pressure profiles along the center line of the channel after 20000 time steps.

In the plot of the pressure difference, the horizontal lines indicate an interval which should contain the pressure value half a period after the lift coefficient has reached its maximum. Like in the other two plots, a phase shift of the signal depending on the aspect ratio is clearly visible.

### 3.2 Extrapolation method

This method has been applied for quite a long time (a recent reference is [28]). To obtain the algorithm, one simply extrapolates the unknown  $f_i$  at a boundary node from the values of two neighboring fluid nodes. Here, we take linear extrapolation which requires two neighboring nodes in the direction of the inner normal, i.e.,

$$f_i(n+1, j_o) = 2f_i(n+1, j_o - \mathbf{n}) - f_i(n+1, j_o - 2\mathbf{n}), \quad (3.8)$$

where again  $j_o$  is the label of a boundary node and  $\mathbf{n}$  is the outer normal direction at the outlet.

To reveal the hydrodynamic outflow condition hidden in this algorithm, we apply the asymptotic analysis. The prediction  $\hat{f}_i$  with coefficients (2.3) is inserted into Eq. (3.8) and

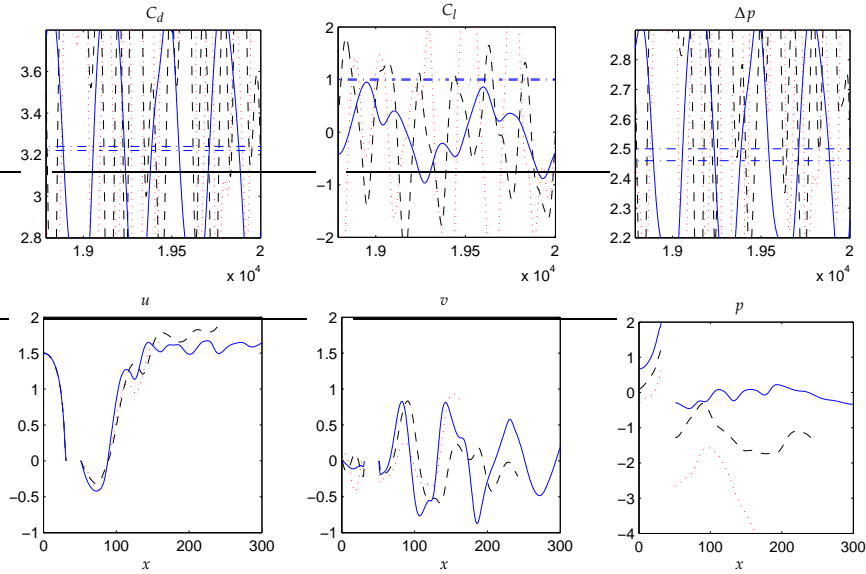


Figure 4: The simulation results obtained with the extrapolation method are demonstrated by the dotted lines ( $L/H=2$ ), dashed lines ( $L/H=3$ ) and solid lines ( $L/H=5$ ). The upper plots show how the drag ( $C_d$ ), lift ( $C_l$ ) coefficients and the pressure difference at cylinder ( $\Delta p$ ) vary in 2000 time steps (from 18000 to 20000). The dash-dotted lines display the interval of the reference values. The lower plots are the velocity and pressure profiles along the center line of the channel after 20000 time steps.

the Taylor expansion around  $(t_n, \mathbf{x}_j)$  leads to

$$h^3 3f_i^* (\mathbf{n} \cdot \nabla)^2 (\mathbf{u} \cdot \mathbf{c}_i) - h^4 3f_i^* \left[ (\mathbf{n} \cdot \nabla)^3 (\mathbf{u} \cdot \mathbf{c}_i) + (\mathbf{n} \cdot \nabla)^2 \left( p + \frac{3}{2} (\mathbf{u} \cdot \mathbf{c}_i)^2 - \frac{1}{2} \mathbf{u}^2 - \tau (\mathbf{c}_i \cdot \nabla) (\mathbf{u} \cdot \mathbf{c}_i) \right) \right] = \mathcal{O}(h^5). \tag{3.9}$$

Taking into account that the incoming velocity directions  $\mathbf{c}_i$  at an outlet node are linearly independent, we can conclude from the leading order term that the second order normal derivative of the fluid velocity vanishes up to terms of order  $h$

$$\frac{\partial^2 \mathbf{u}}{\partial n^2} = \mathcal{O}(h). \tag{3.10}$$

The simulation results of the test flow based on the extrapolation condition are displayed in Fig. 4. Obviously, the outflow condition strongly deteriorates the flow in the interior. The maximum of the drag and lift coefficients as well as the pressure difference at the cylinder are far away from the reference intervals even for the large aspect ratio  $L/H=5$ . Also, the velocity and pressure profiles along the center line of the channel strongly depend on the ratio  $L/H$ . These results indicate that the outflow condition

$$\frac{\partial^2 \mathbf{u}}{\partial n^2} = 0 \tag{3.11}$$

induced, in leading order, by the extrapolation method does not fit well to the Navier-Stokes equation for incompressible fluid flow.

However, a condition similar to (3.11) is discussed in the literature [4–6]. In these articles, general outflow boundary conditions of the form

$$\frac{\partial^j \mathbf{u} \cdot \mathbf{n}}{\partial \mathbf{n}^j} = 0, \quad \frac{\partial^q \mathbf{u} \cdot \mathbf{t}}{\partial \mathbf{n}^q} = 0, \quad p = p_0 \tag{3.12}$$

are investigated with respect to the formation of boundary layers (the analysis is based on Laplace-Fourier techniques applied to the linearized, time-dependent Navier-Stokes equations). The authors show that outflow boundary layers are weaker for higher values of  $j$  and  $q$ . Moreover, the choice  $j = q + 1$  leads to divergence free solutions, while the case  $j \neq q + 1$  leads to a divergence production that is confined to the boundary layer when the viscosity is small. They recommend using  $j = 3$  and  $q = 2$  and consider  $j = 2, q = 2$  as acceptable for small viscosities.

The latter case, however, almost corresponds to condition (3.11) with the only difference that the pressure condition in (3.12) is missing. To fix this problem, we propose a modification of the extrapolation method which also incorporates a pressure Dirichlet condition. Noting that the condition (3.4) originating from the algorithm (3.2a) implies  $p = 0$  if we formally set  $\nu = 0$ , we are led to

$$f_i(n+1, \mathbf{j}_0) = [F_i^{eq}(1, \hat{\mathbf{u}}) + f_{i*}^{neq}](n, \mathbf{j}_0), \quad \mathbf{c}_i = -\mathbf{n}, \tag{3.13a}$$

$$f_i(n+1, \mathbf{j}_0) = 2f_i(n+1, \mathbf{j}_0 - \mathbf{n}) - f_i(n+1, \mathbf{j}_0 - 2\mathbf{n}), \quad \mathbf{c}_i \neq -\mathbf{n}, \tag{3.13b}$$

where the extrapolation condition is kept for the non-normal velocity directions. The

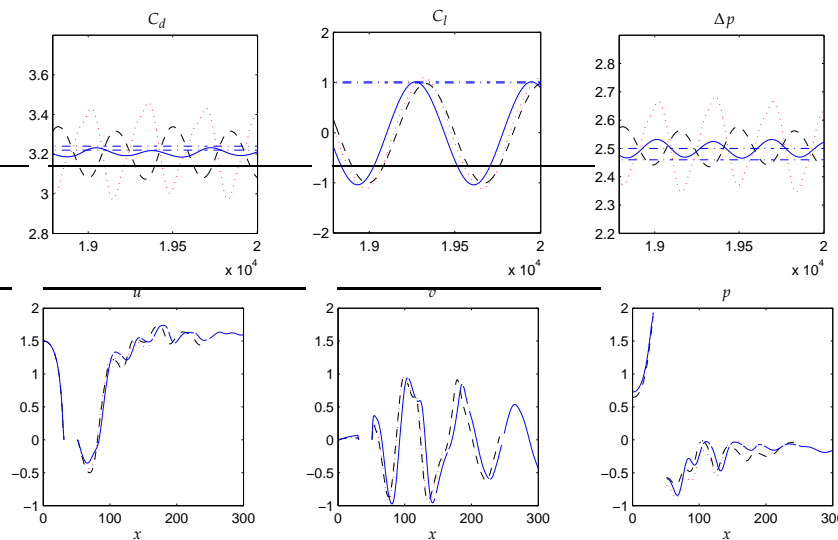


Figure 5: The simulation results obtained with the modified extrapolation algorithm are demonstrated by the dotted lines ( $L/H=2$ ), dashed lines ( $L/H=3$ ) and solid lines ( $L/H=5$ ). The upper plots show how the drag ( $C_d$ ), lift ( $C_l$ ) coefficients and the pressure difference at cylinder ( $\Delta p$ ) vary in 2000 time steps (from 18000 to 20000). The dash-dotted lines display the interval of the reference values. The lower plots are the velocity and pressure profiles along the center line of the channel after 20000 time steps.

asymptotic analysis shows that this algorithm is consistent to the boundary conditions

$$\frac{\partial^2 \mathbf{u}}{\partial n^2} = 0, \quad p = 0, \quad (3.14)$$

which are a special case of (3.12) with  $j=q=2$  and  $p_0=0$ . The simulation results obtained with the modified extrapolation scheme are displayed in Fig. 5. We observe a dramatic improvement compared to the original extrapolation method. The results are now comparable to those obtained with the do-nothing condition.

## 4 Discussion and conclusions

We have taken two lattice Boltzmann outflow algorithms, the extrapolation method [28] and the do-nothing condition [19], as representatives of two types of outflow treatments. The do-nothing condition is originally given in terms of the hydrodynamical variables [24] and requires the construction of a corresponding lattice Boltzmann algorithm. Conversely, in the case of the extrapolation method, the lattice Boltzmann algorithm is constructed first and the question concerning the induced hydrodynamical condition arises which eventually leads to conditions reported in [4–6].

In both scenarios, the asymptotic analysis is a valuable tool. The explicit knowledge of the relation between Navier-Stokes fields and leading order contributions to the lattice Boltzmann variables helps in designing algorithms for given boundary conditions, and afterward, allows to estimate the resulting accuracy. The analysis of the extrapolation method, on the other hand, is a nice example how gained insight into the hydrodynamical consequences of a given algorithm can lead to successful improvements.

## References

- [1] T. Abe, Derivation of the lattice Boltzmann method by means of the discrete ordinate method for the Boltzmann equation, *J. Comput. Phys.*, 131 (1997), 241–246.
- [2] R. Benzi, S. Succi, and M. Vergassola, The lattice-Boltzmann equation: theory and applications, *Phys. Rep.*, 222 (1992), 145–197.
- [3] S. S. Chikatamarla, S. Ansumali, and I. V. Karlin, Grad’s approximation for missing data in lattice Boltzmann simulations, *Europhys. Lett.*, 74(2) (2006), 215–221.
- [4] B. Christer and V. Johansson, Well-posedness in the generalized sense for boundary layer suppressing boundary conditions, *J. Sci. Comput.*, 6-4 (1991), 391–414.
- [5] B. Christer and V. Johansson, Well-posedness in the generalized sense for the incompressible Navier-Stokes equation, *J. Sci. Comput.*, 6-2 (1991), 101–127.
- [6] B. Christer and V. Johansson, Boundary conditions for open boundaries for the incompressible Navier-Stokes equation, *J. Comput. Phys.*, 105 (1993), 233–251.
- [7] S. Blazy, S. Nazarov and M. Specovius-Neugebauer, Artificial boundary conditions of pressure type for viscous flows in a system of pipes, *J. Math. Fluid. Mech.*, 9 (2007), 1–33.
- [8] D. d’Humières, Generalized lattice-Boltzmann equations. in rarefied gas dynamics: theory and simulations, (eds. B. D. Shizgal and D. P. Weaver), *Progr. Astronaut. Aero.*, 59 (1992), 450–548.

- [9] D. d’Humières, I. Ginzbourg, M. Krafczyk, P. Lallemand, and L.-S. Luo, Multiple-relaxation-time lattice Boltzmann models in three dimensions, *Phil. Trans. R. Soc. Lond. A.*, 360 (2002), 437–451.
- [10] U. Frisch, D. d’Humières, B. Hasslacher, P. Lallemand, Y. Pomeau, and J. P. Rivet, Lattice gas hydrodynamics in two and three dimensions, *Complex. Sys.*, 1 (1987), 649–707.
- [11] X. He and L.-S. Luo, A priori derivation of the lattice Boltzmann equation, *Phys. Rev. E.*, 55 (1997), 6333–6336.
- [12] X. He and L.-S. Luo, Lattice Boltzmann model for the incompressible Navier-Stokes equation, *J. Stat. Phys.*, 88(3/4) (1997), 927–944.
- [13] X. He and L.-S. Luo, Theory of the lattice Boltzmann method: from the Boltzmann equation to the lattice Boltzmann equation, *Phys. Rev. E.*, 56 (1997), 6811–6817.
- [14] J. Heywood, R. Rannacher, and S. Turek, Artificial boundaries and flux and pressure conditions for the incompressible Navier–Stokes equations, *Int. J. Numer. Math. Fluids.*, 22 (1996), 325–352.
- [15] F. Higuera and J. Jiménez, Boltzmann approach to lattice gas simulations, *Europhys. Lett.*, 9 (1989), 663.
- [16] S. Izquierdo, P. Martinez-Lera, and N. Fueyo, Analysis of open boundary effects in unsteady lattice Boltzmann simulations, *Comput. Math. Appl.*, doi:10.1016/j.camwa.1009.02.014 (2009).
- [17] M. Junk, A. Klar, and L.-S. Luo, Asymptotic analysis of the lattice Boltzmann equation, *J. Comput. Phys.*, 210 (2005), 676–704.
- [18] M. Junk and Z. Yang, Asymptotic analysis of lattice Boltzmann boundary conditions, *J. Stat. Phys.*, 121 (2005), 3–35.
- [19] M. Junk and Z. Yang, Outflow boundary conditions for the lattice Boltzmann method, *Progr. Comput. Fluid. Dyn.*, 8 (2008), 38–48.
- [20] P. Lallemand and L.-S. Luo, Theory of the lattice Boltzmann method: dispersion, dissipation, isotropy, Galilean invariance, and stability, *Phys. Rev. E.*, 61 (2000), 6546–6562.
- [21] G. McNamara and G. Zanetti, Use of Boltzmann equation to simulate lattice-gas automata, *Phys. Rev. Lett.*, 61 (1988), 2332.
- [22] Y. Qian, Lattice Gas and Lattice Kinetic Theory Applied to the Navier-Stokes Equations, PhD thesis, 1990.
- [23] Y. Qian, D. d’Humières, and P. Lallemand, Lattice BGK models for Navier-Stokes equation, *Europhys. Lett.*, 17 (1992), 479–484.
- [24] M. Schäfer and S. Turek, Benchmark computations of laminar flow around a cylinder, in *Flow simulation with high-performance computers II*, Volume 52 of notes on numerical fluid dynamics, Viehweg, I. E. Hirschel, ed., 1996, 547–566.
- [25] F. Verhaeghe, L.-S. Luo, and B. Blanpain, Lattice Boltzmann modeling of microchannel flow in slip flow regime, *J. Comput. Phys.*, 228 (2009), 147–157.
- [26] Z. Yang, Lattice Boltzmann outflow treatments: convective conditions and others, to appear.
- [27] Z. Yang., Analysis of Lattice Boltzmann Boundary Conditions, Dissertation, Uni. Konstanz, 2007.
- [28] D. Yu, R. Mei, and W. Shyy, Improved treatment of the open boundary in the method of lattice Boltzmann equation, *Progr. Comput. Fluid. Dyn.*, 5(1/2) (2005), 1–11.